A nearly complete census of intergalactic gas using the kSZ effect

Sixteenth Marcel Grossmann Meeting
06/07/21

Jonás Chaves-Montero
Donostia International Physics Center
jonas.chaves@dipc.org

Monthly Notices
of the
ROYAL ASTRONOMICAL SOCIETY

MNRAS **503,** 1798–1814 (2021) doi:10.1093/mnras/staa3782

Measuring the evolution of intergalactic gas from $z = 0$ to 5 using the kinematic Sunyaev–Zel'dovich effect

Jonás Chaves-Montero ,[1,2,3★] Carlos Hernández-Monteagudo,[4] Raúl E. Angulo[3,5] and J. D. Emberson[6]

[1] *HEP Division, Argonne National Laboratory, 9700 South Cass Avenue, Lemont, IL 60439, USA*

[2] *Centro de Estudios de Física del Cosmos de Aragón, Plaza San Juan 1, Planta-3, E-44001 Teruel, Spain*

[3] *Donostia International Physics Centre, Paseo Manuel de Lardizabal 4, E-20018 Donostia-San Sebastian, Spain*

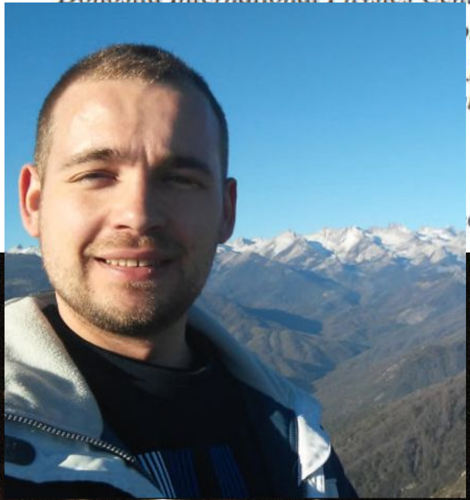

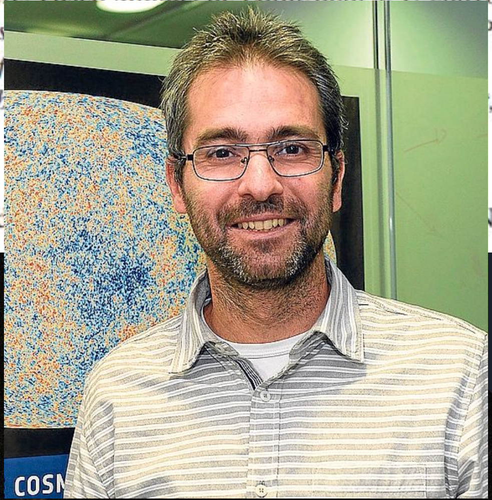

Composition of the Universe

Three main components today:

- Dark Energy
- Dark Matter
- Baryonic Matter

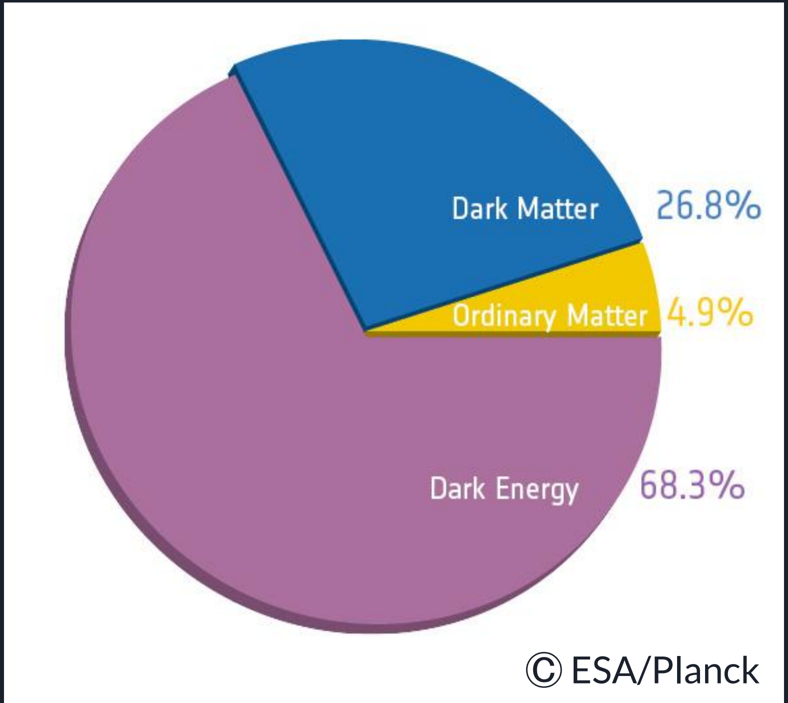

Composition of the Universe

Three main components today:

- Dark Energy (unknown)
- Dark Matter (unknown)
- Baryonic Matter (under control, right?)

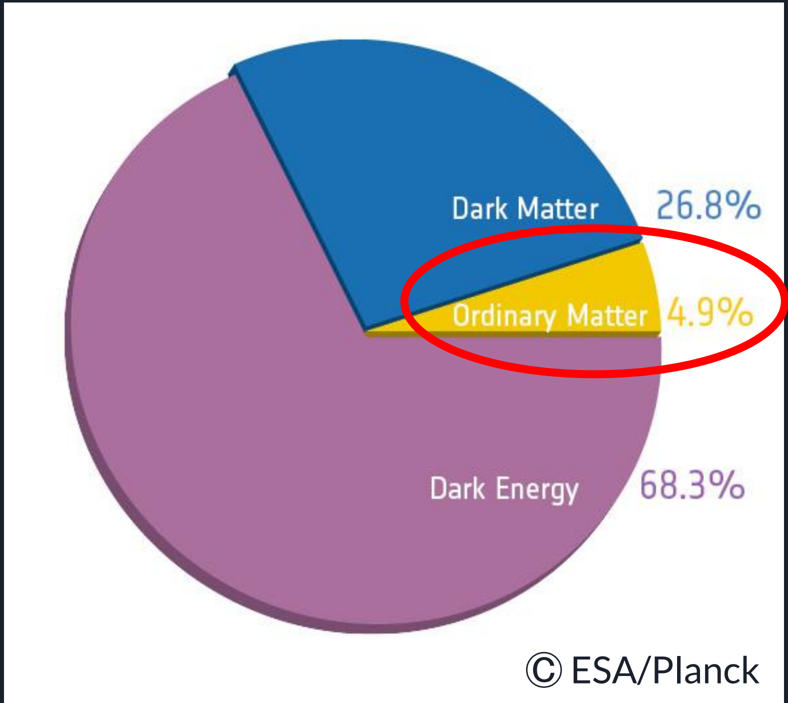

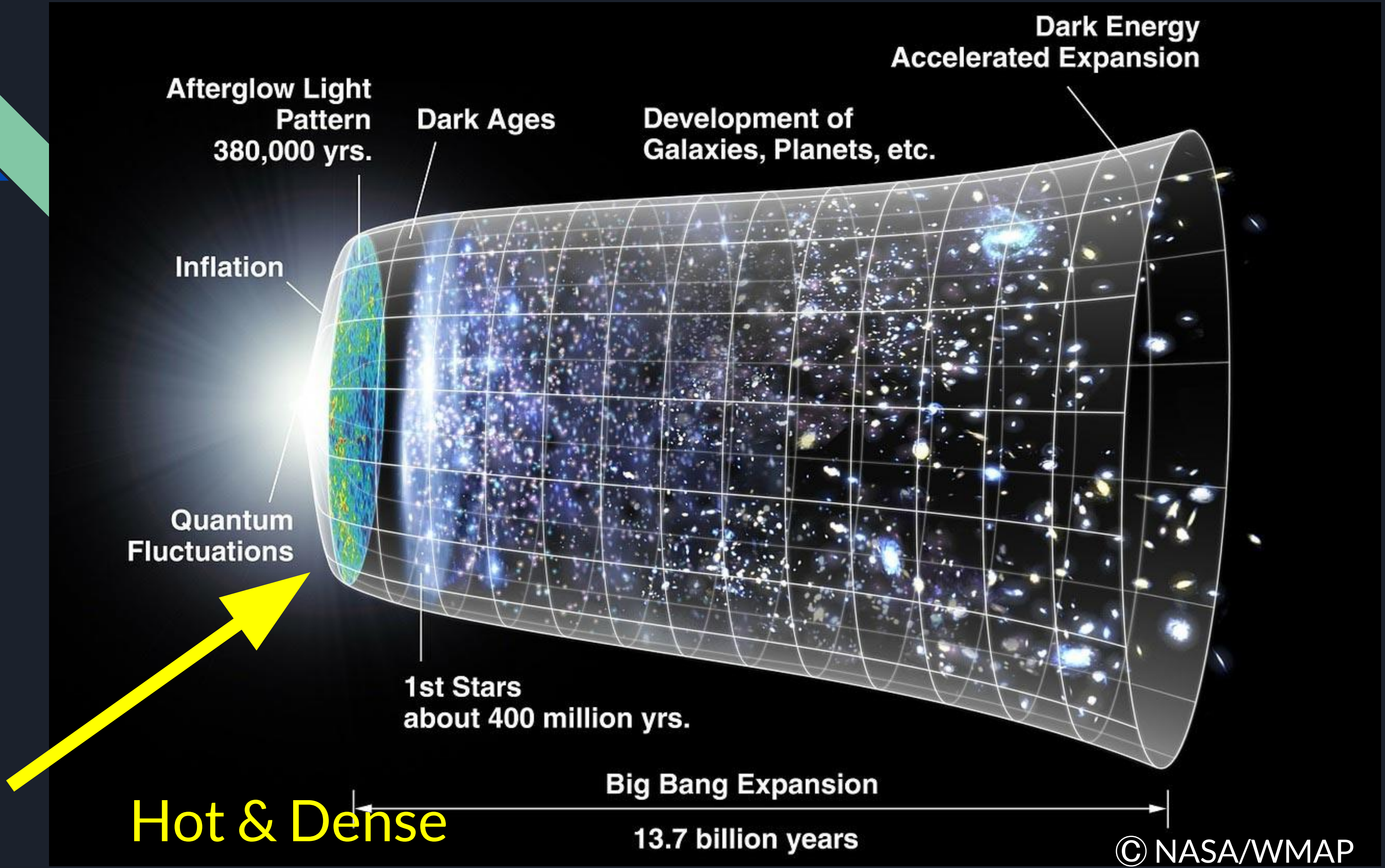
Dark Energy
Accelerated Expansion
Afterglow Light
Pattern
380,000 yrs.
Dark Ages
Development of
Galaxies, Planets, etc.
Inflation
Quantum
Fluctuations
1st Stars
about 400 million yrs.
Big Bang Expansion
13.7 billion years
Hot & Dense
© NASA/WMAP

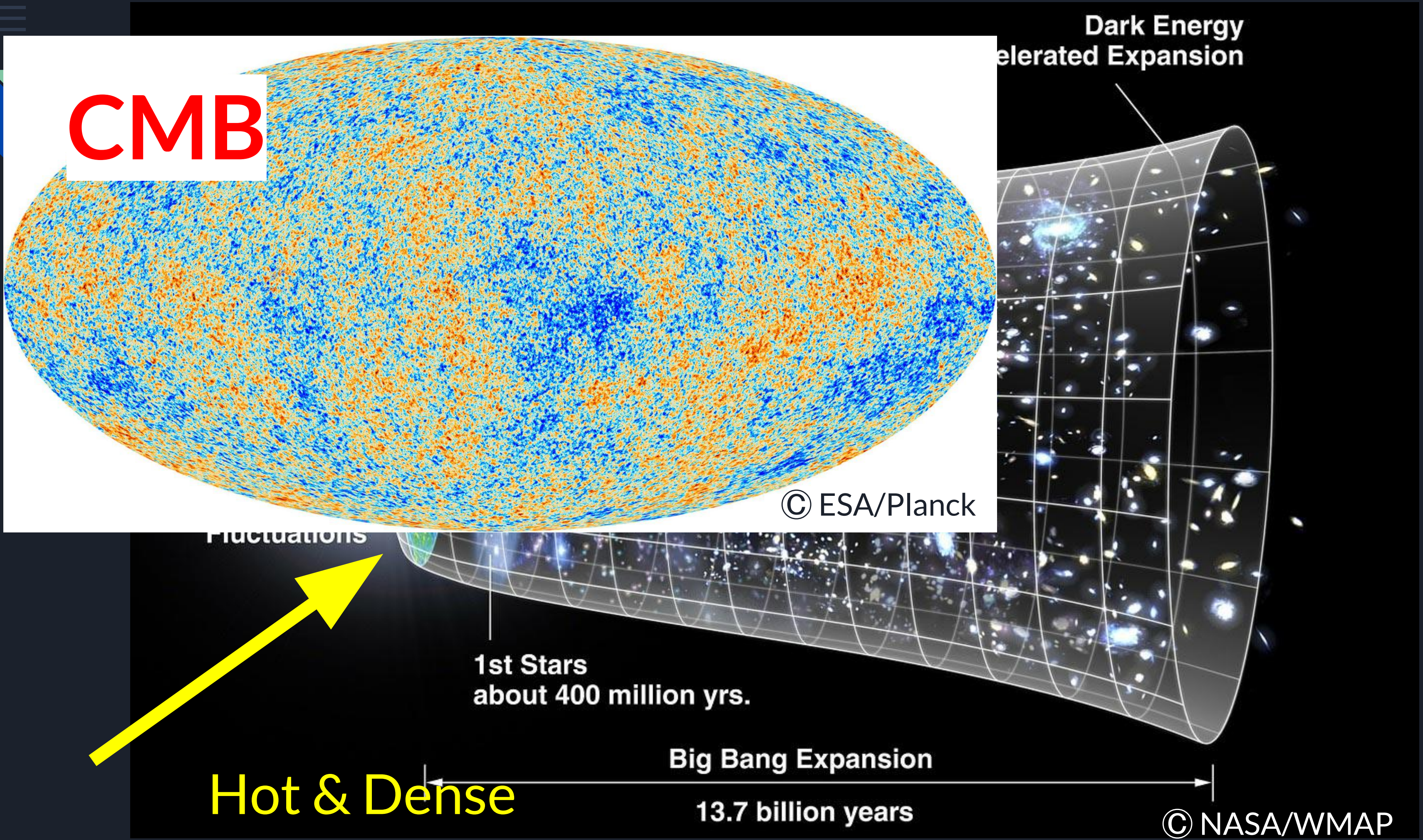
Dark Energy
elerated Expansion
Fluctuations
1st Stars
about 400 million yrs.
Big Bang Expansion
13.7 billion years
© NASA/WMAP
CMB
© ESA/Planck

Hot & Dense

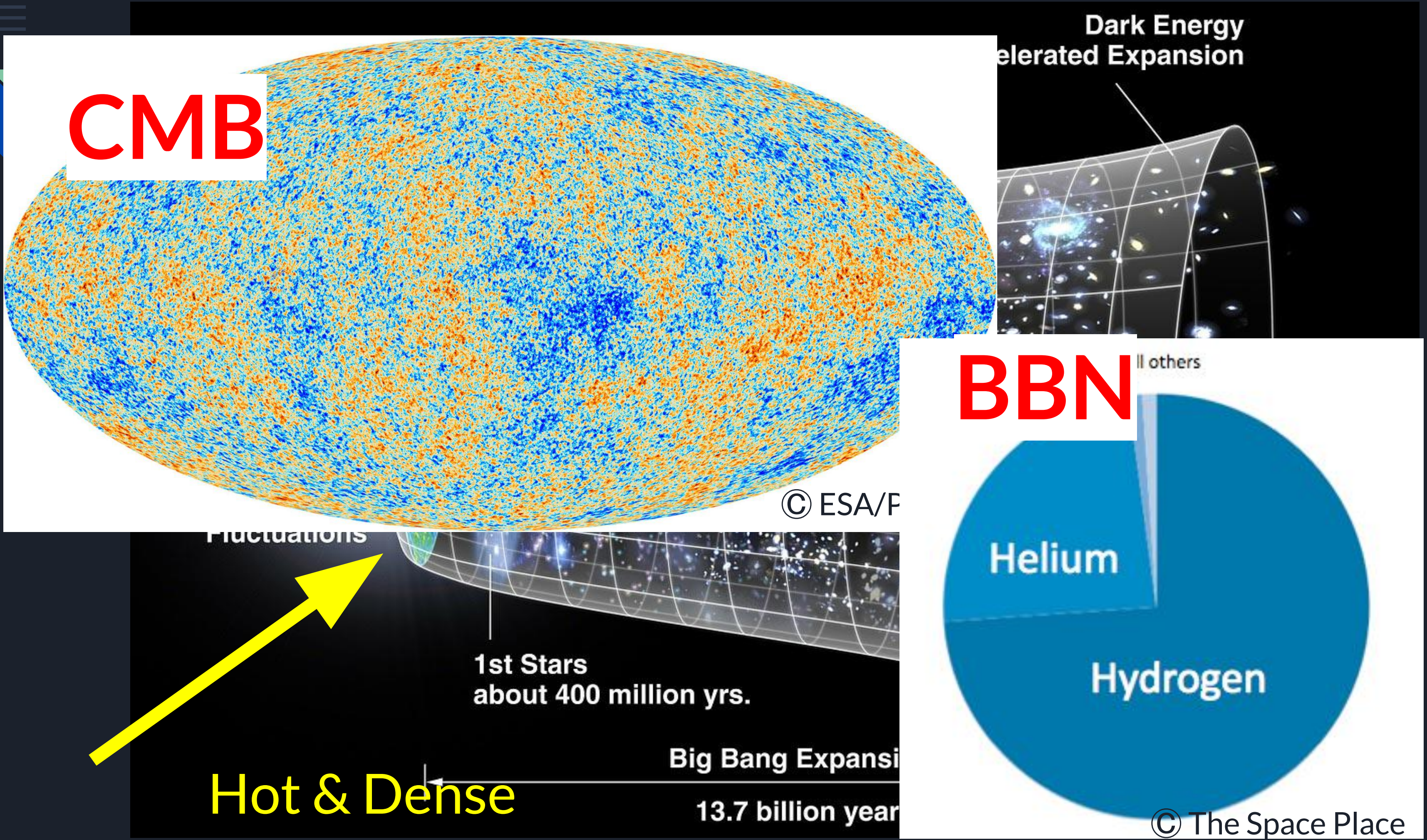
CMB
© ESA/P
Dark Energy
elerated Expansion
1st Stars
about 400 million yrs.
Big Bang Expansi
13.7 billion year
Hot & Dense
BBN
ll others
Helium
Hydrogen
© The Space Place

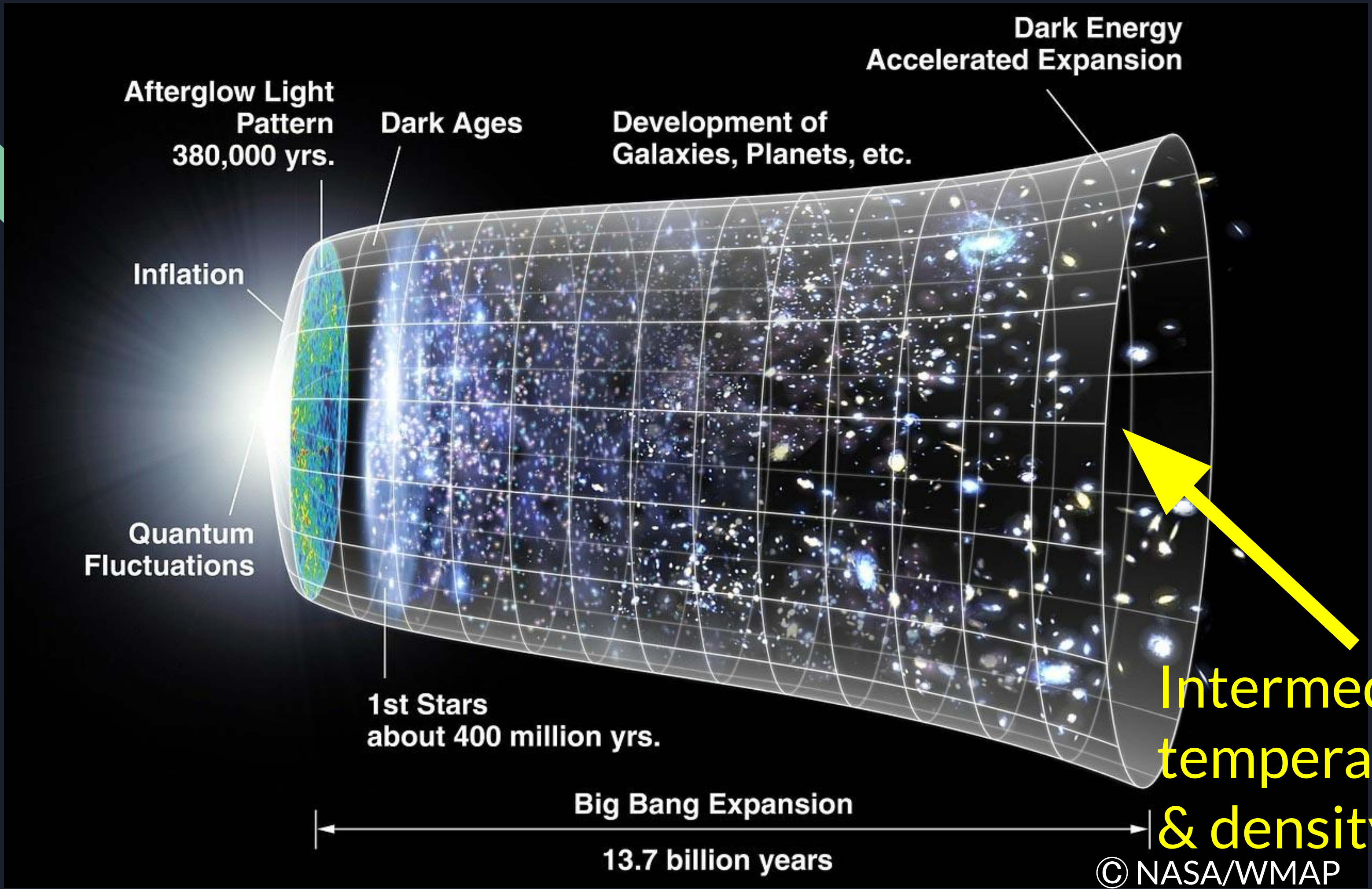

Intermediate temperature & density

Missing baryon problem

Location of baryons:

- Galaxies (stars, gas, etc.)
- Intracluster and circumgalactic medium
- Intergalactic medium

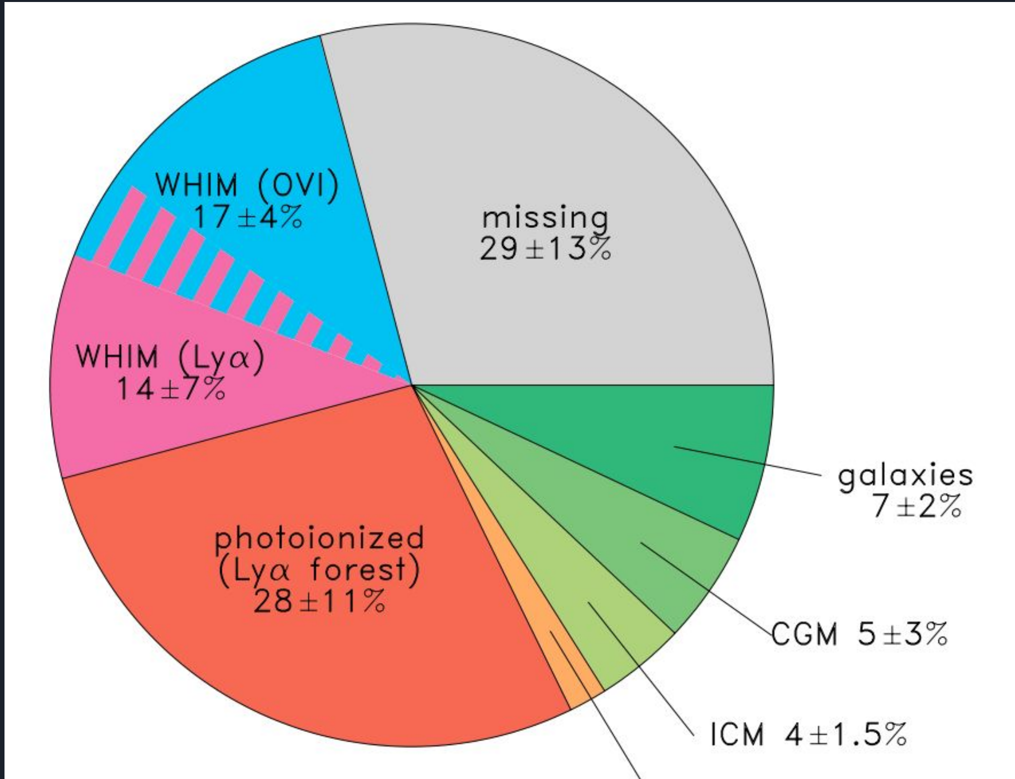

© Shull+ 2012

Intergalactic medium

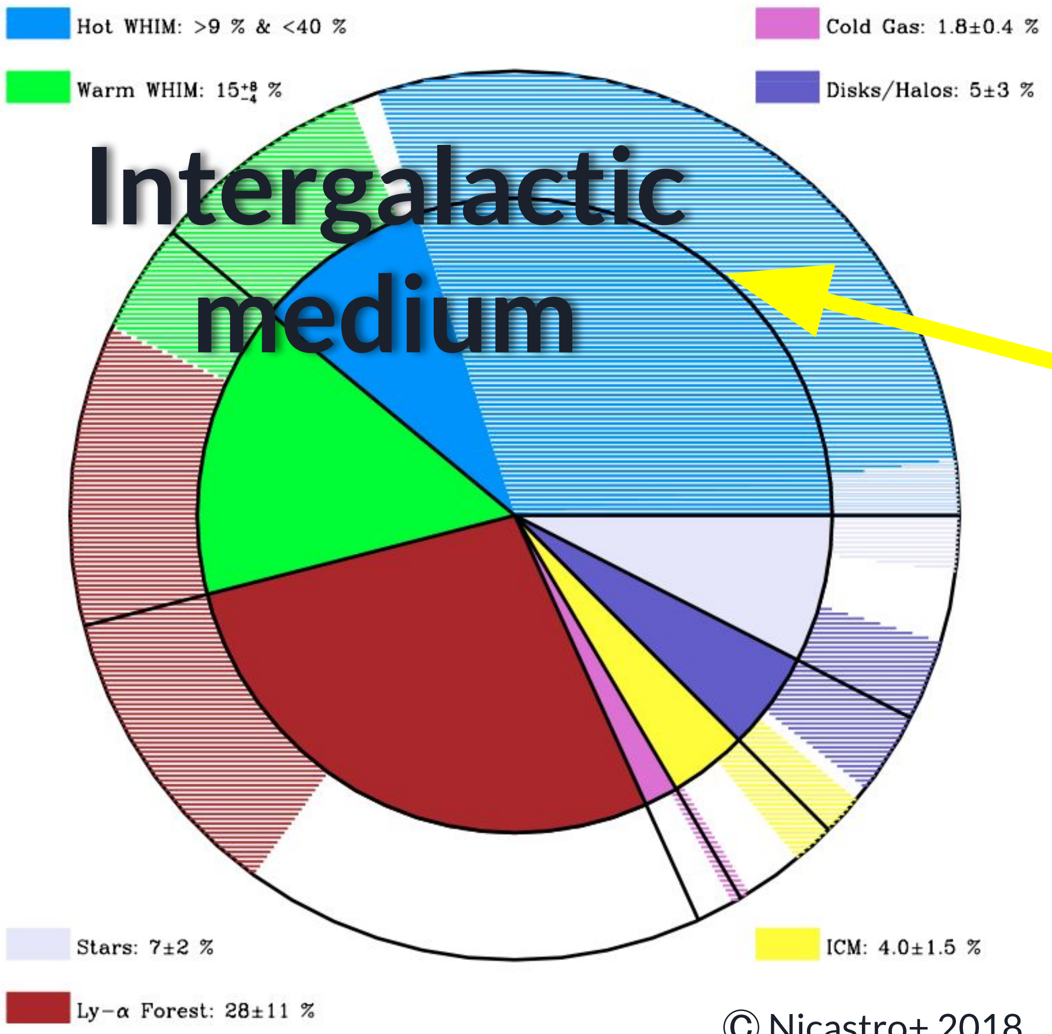

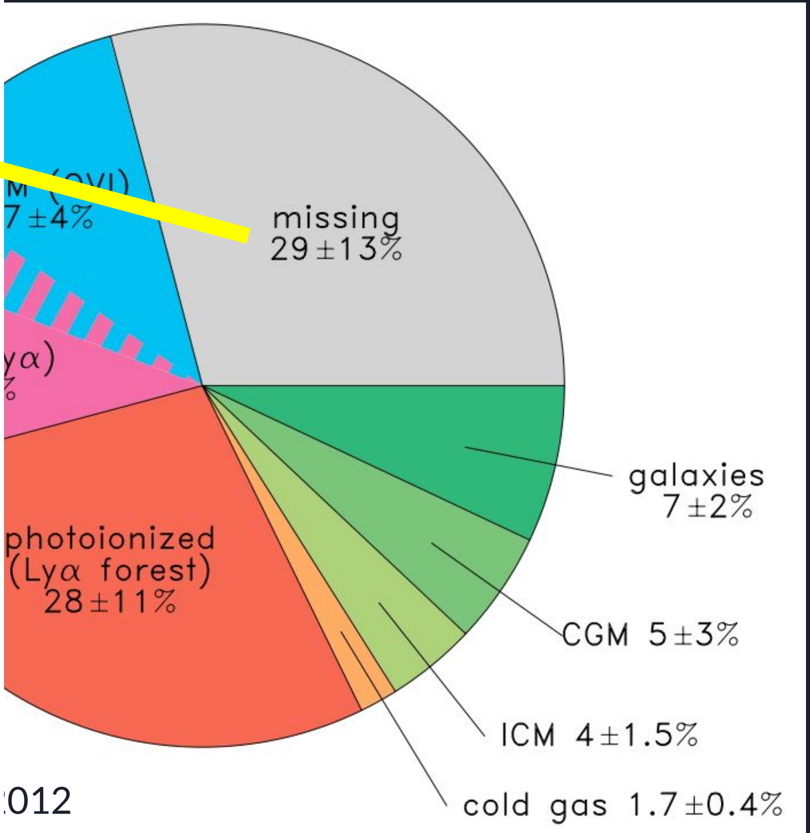

012

© Nicastro+ 2018

Solving the missing baryon problem (I)

Kinematic Sunyaev-Zel'dovich effect

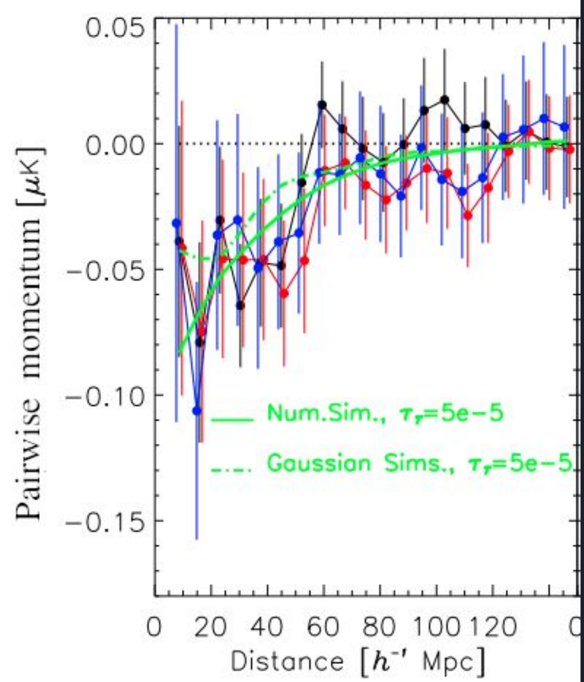

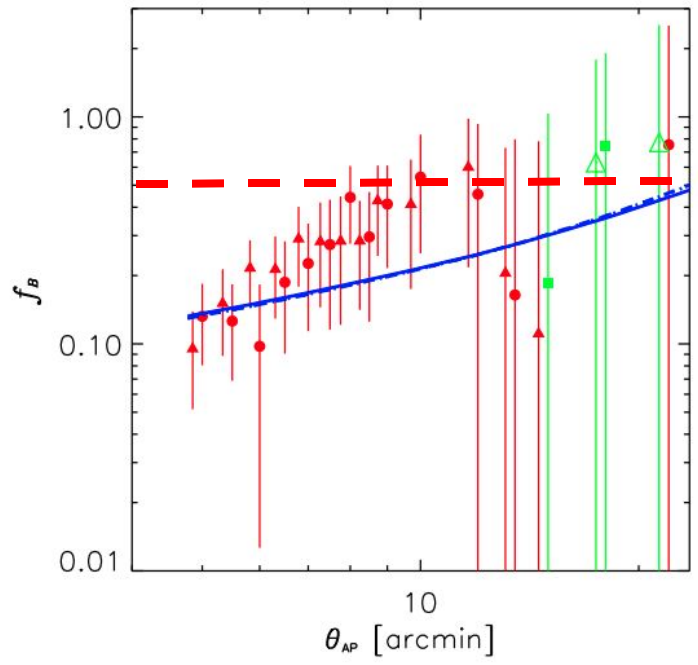

Hernández-Monteagudo+2015

Solving the missing baryon problem (II)

Deep X-ray observations

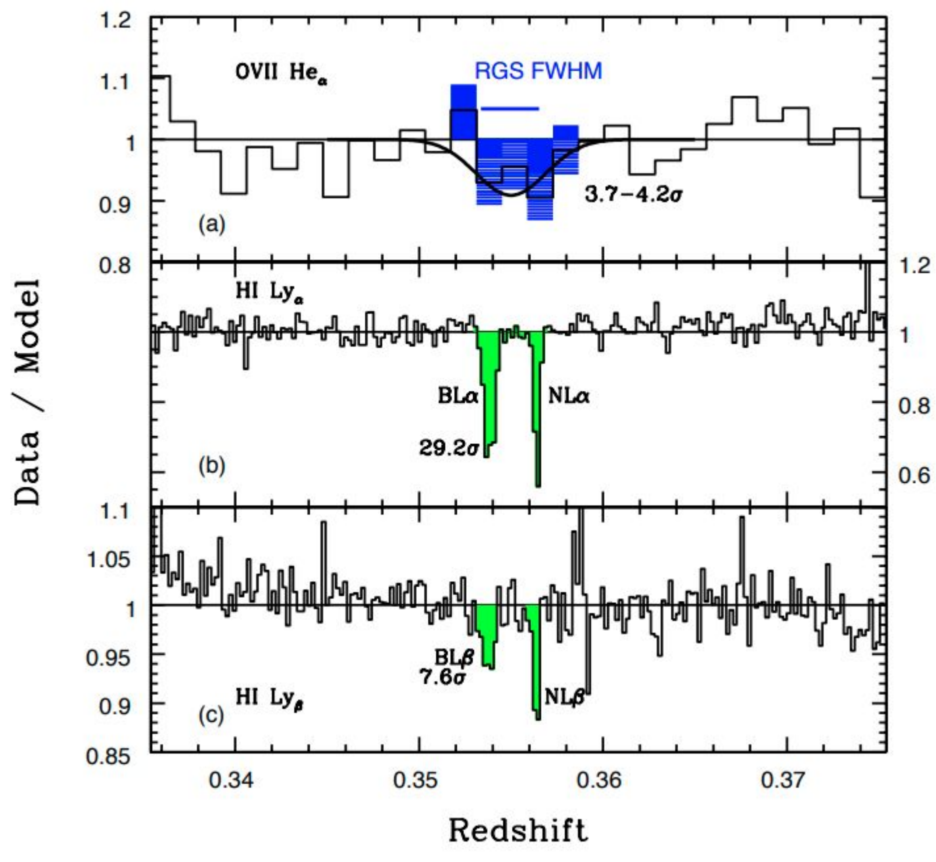

Nicastro+2018

Solving the missing baryon problem (III)

Thermal Sunyaev-Zel'dovich effect

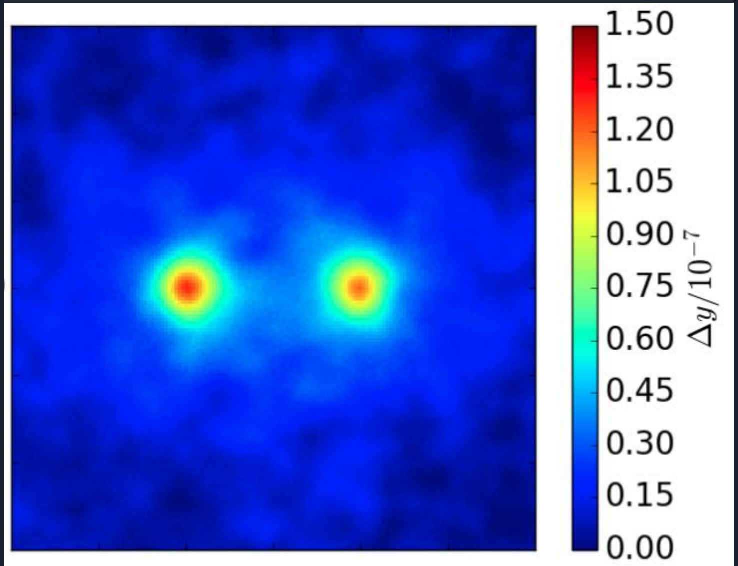

Tanimura+2019

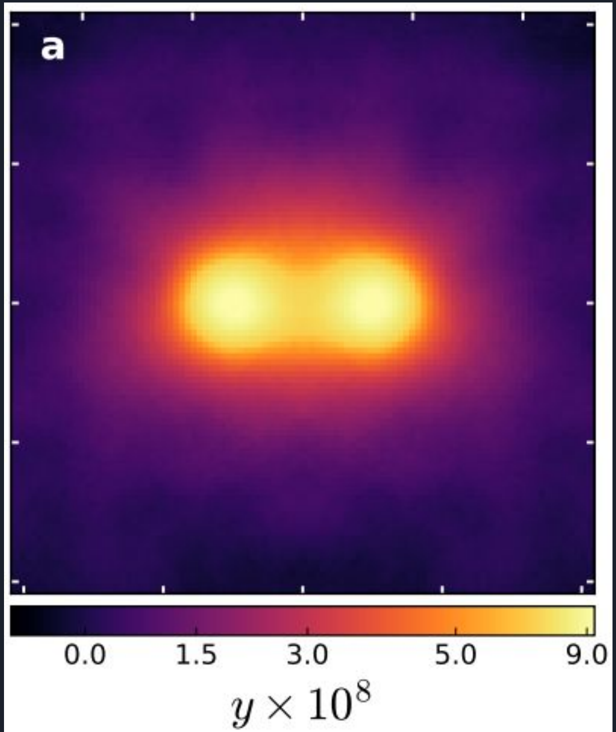

de Graaff+2019

Status of the problem

All these works set constraints on the distribution of cosmic baryons at either a few specific redshifts or across a reduced number of line-of-sights

A complete picture of cosmic gas at late times is **still missing**

Methods to detect intergalactic gas:

- Deep X-ray campaigns
- Lyman-α forest
- Thermal Sunyaev-Zel'dovich effect
- Kinematic Sunyaev-Zel'dovich effect (kSZ effect)

Kinematic Sunyaev-Zel'dovich effect (I)

Doppler boosting of CMB photons as these scatter off free electrons moving relative to the CMB rest frame (Sunyaev & Zel'dovich 1972, 1980)

$$\frac{\Delta T}{T} = -\sigma_T \int \mathrm{d}l \, n \frac{v_{||}}{c}$$

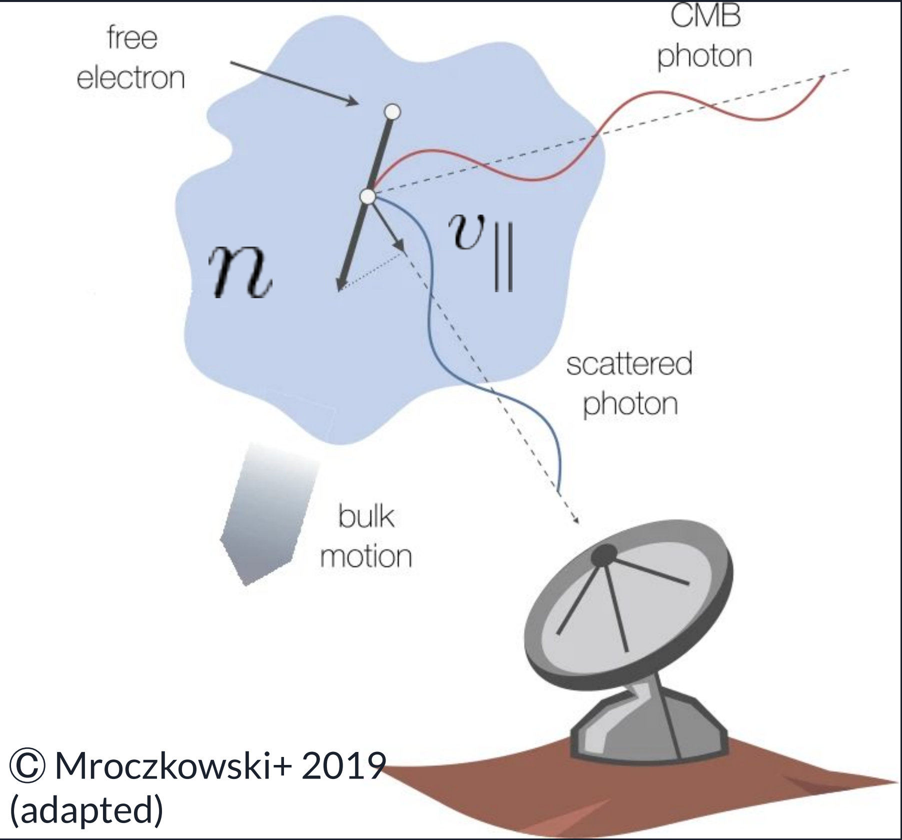

Kinematic Sunyaev-Zel'dovich effect (II)

The kSZ effect is sensitive to all free electrons, independently of the temperature and density of their medium

Detecting the kSZ effect is challenging due to its:

- Spectral shape
- Amplitude

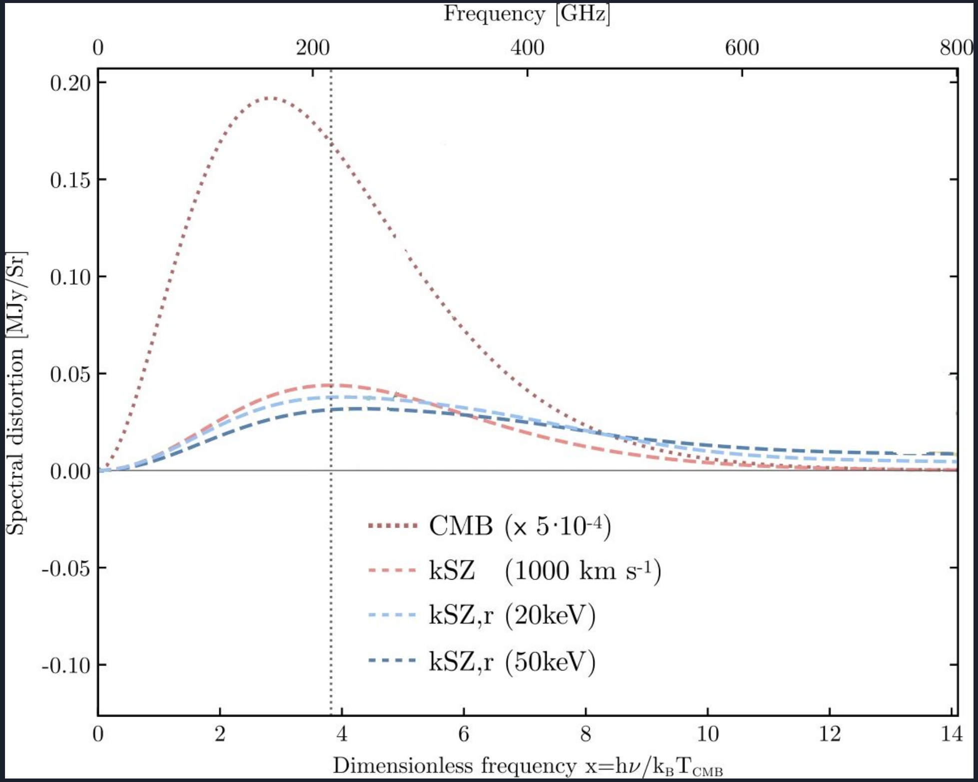

© Mroczkowski+ 2019 (adapted)

ARF-kSZ tomography (I)

ARF-kSZ tomography: cross-correlation of CMB observations and angular fluctuations in the galaxy redshift field

$$\mathcal{Z}^{2D}(\hat{\Omega}) = \int \mathrm{d}s\, s^2 \left[z + (1+z)\frac{v}{c} \right] W(s)\, n(\mathbf{s}),$$

Broad window □ ARF sensitive to density field
Narrow window □ ARF sensitive to velocity field

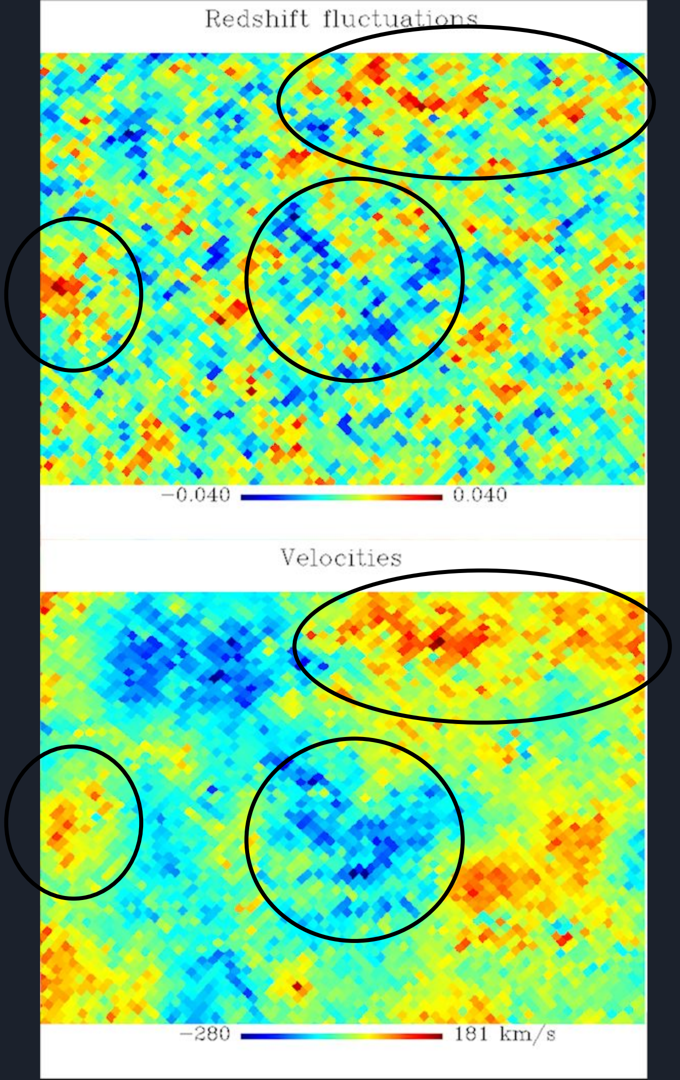

ARF-kSZ tomography (II)

kSZ effect proportional to the cosmic velocity field

ARF sensitive to the cosmic velocity field

Cross-correlation of ARF and CMB observations to extract the kSZ effect

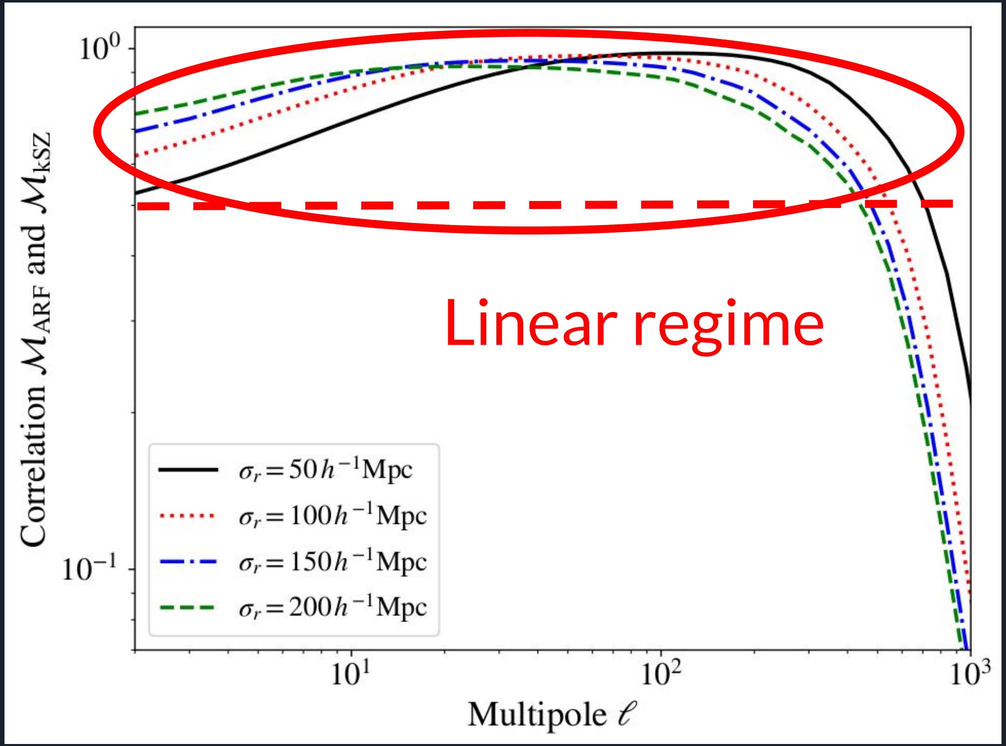

Chaves-Montero+2021

Data

CMB observations

Foreground-reduced Planck temperature maps (all sky):

COMMANDER, NILC, SEVEM, SMICA, SMICA-NOSZ, SEVEM-100, SEVEM-143, SEVEM-217

Large-scale structure tracers

6dF galaxies (1 shell, 50% of the sky): z_{cen}=0.18

BOSS galaxies (4 shells, 25% of the sky): z_{cen}=0.27, 0.42, 0.59, and 0.78

SDSS QSOs (11 shells, 25% of the sky): z_{cen}=0.72, 0.92, 1.2, 1.4, 1.7, 2.1, 2.5, 3.0, 3.6, 4.4, and 5.4

Problem: primordial CMB fluctuations

We apply an aperture photometry filter to CMB observations on the sky coordinates of each galaxy

This technique removes temperature fluctuations constant over the filter aperture, alleviating the contamination from primordial CMB anisotropies

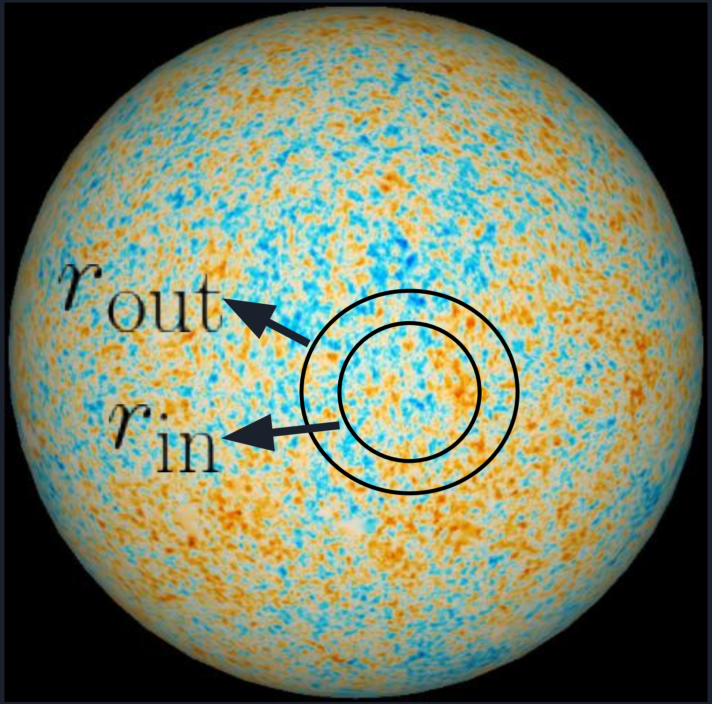

ARF-kSZ tomography: summary

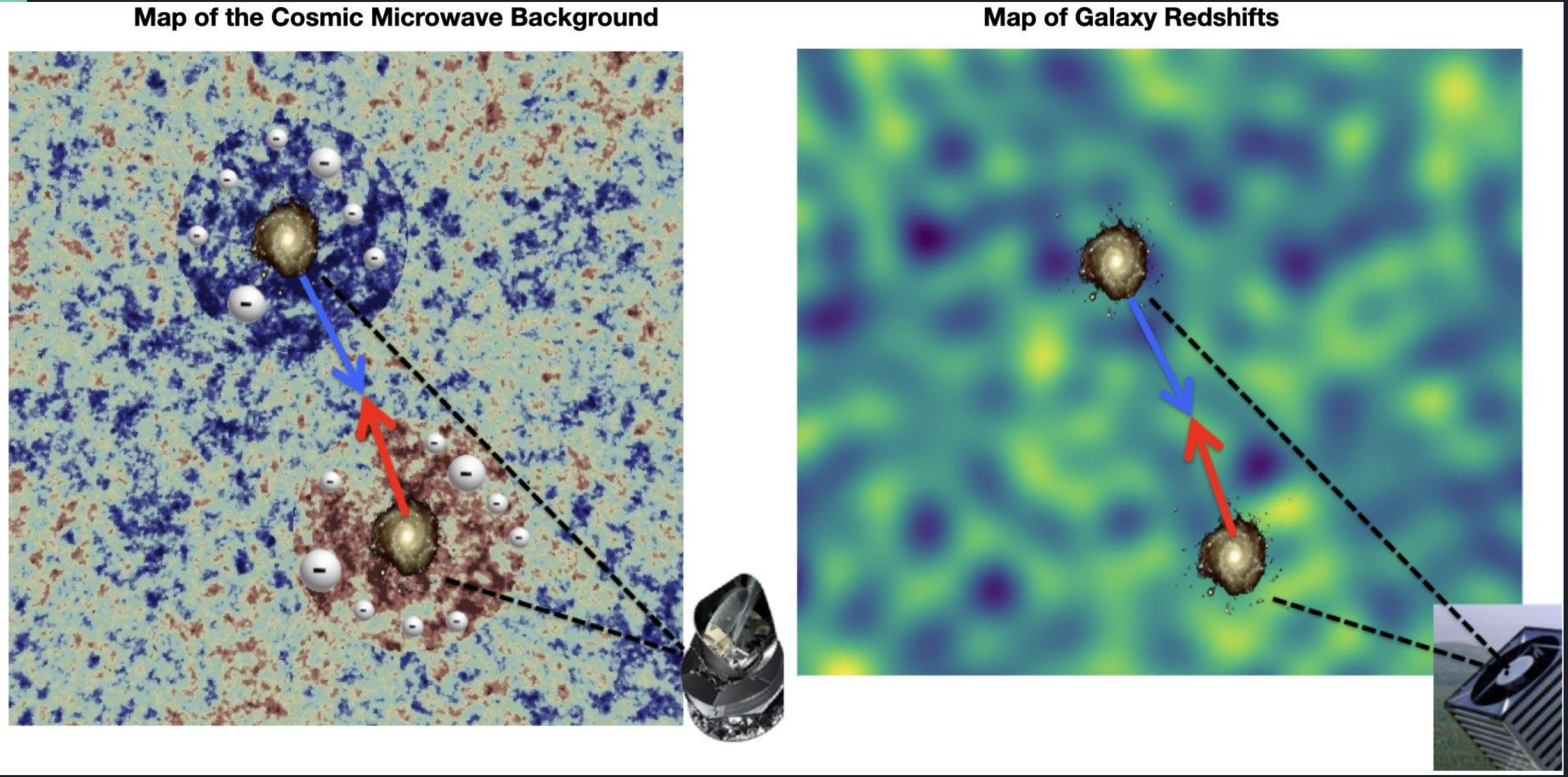

ARF-kSZ tomography: results

BOSS galaxies at *z*=0.56

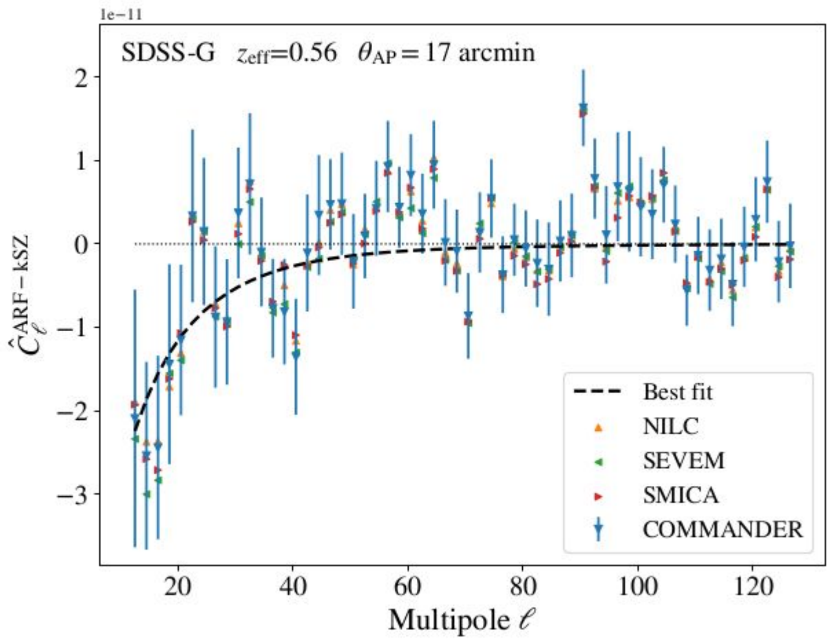

SDSS quasars at *z*=4.03

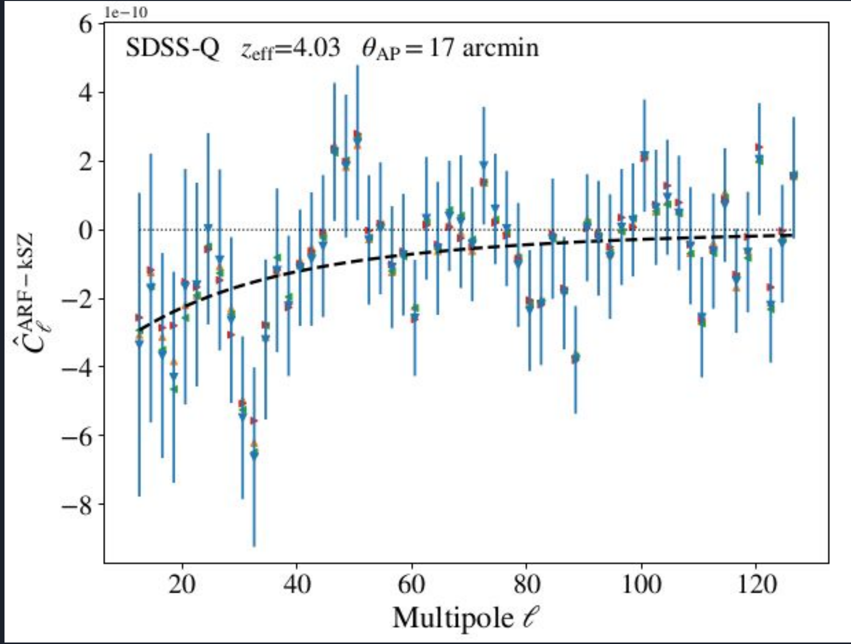

Chaves-Montero+2021

ARF-kSZ tomography: significance

We detect cross-correlation for most redshift shells and apertures

After accounting for correlations between shells and apertures, 11.4±1.4σ detection of the kSZ effect

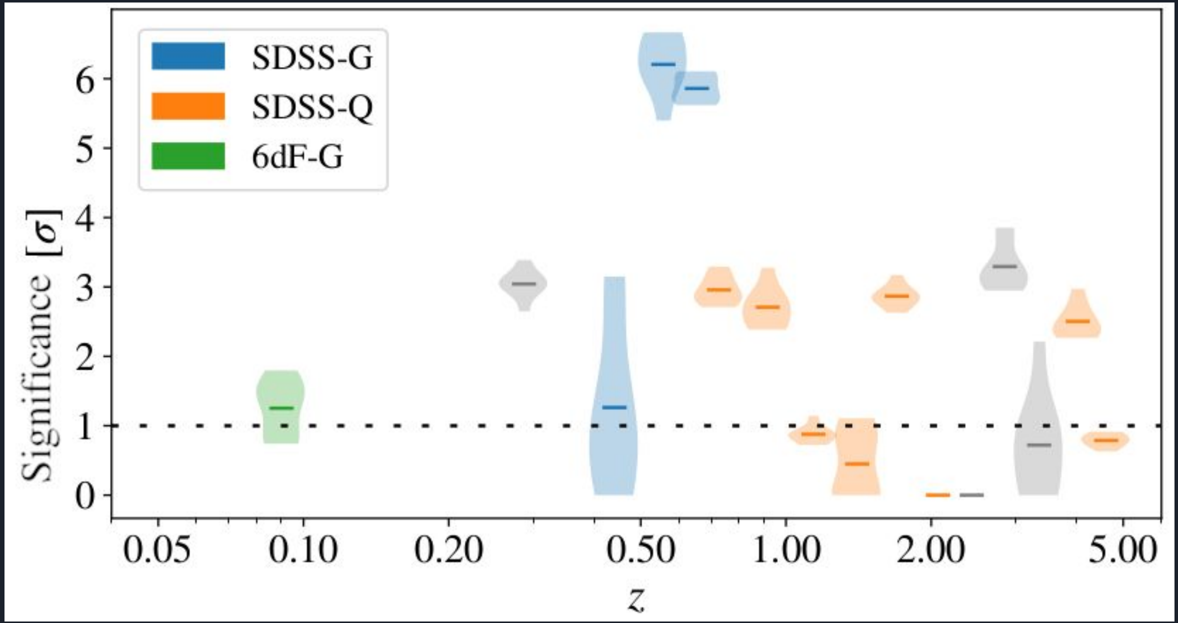

Chaves-Montero+2021

Extracting kSZ optical depth

We extract the kSZ optical depth from the cross-correlation of maps:

$$\tau_{\mathrm{AP}}(\theta_{\mathrm{AP}}) = \frac{\sum_{\ell\ell'} \hat{C}_{\ell}^{\mathrm{ARF-kSZ}}(\theta_{\mathrm{AP}}) C_{\ell\ell'}^{-1}(\theta_{\mathrm{AP}}) C_{\ell'}^{\mathrm{cr}}}{\sum_{\ell\ell'} C_{\ell}^{\mathrm{cr}} C_{\ell\ell'}^{-1}(\theta_{\mathrm{AP}}) C_{\ell'}^{\mathrm{cr}}},$$

- Covariance matrix from the cross-correlation of observed ARF maps and simulated CMB maps
- C^{cr} from linear perturbation theory

Redshift evolution of kSZ optical depth

The black (red) dashed line indicates theoretical predictions assuming that 100% (50%) of cosmic baryons contribute to the signal

Data and predictions show comparable redshift evolution

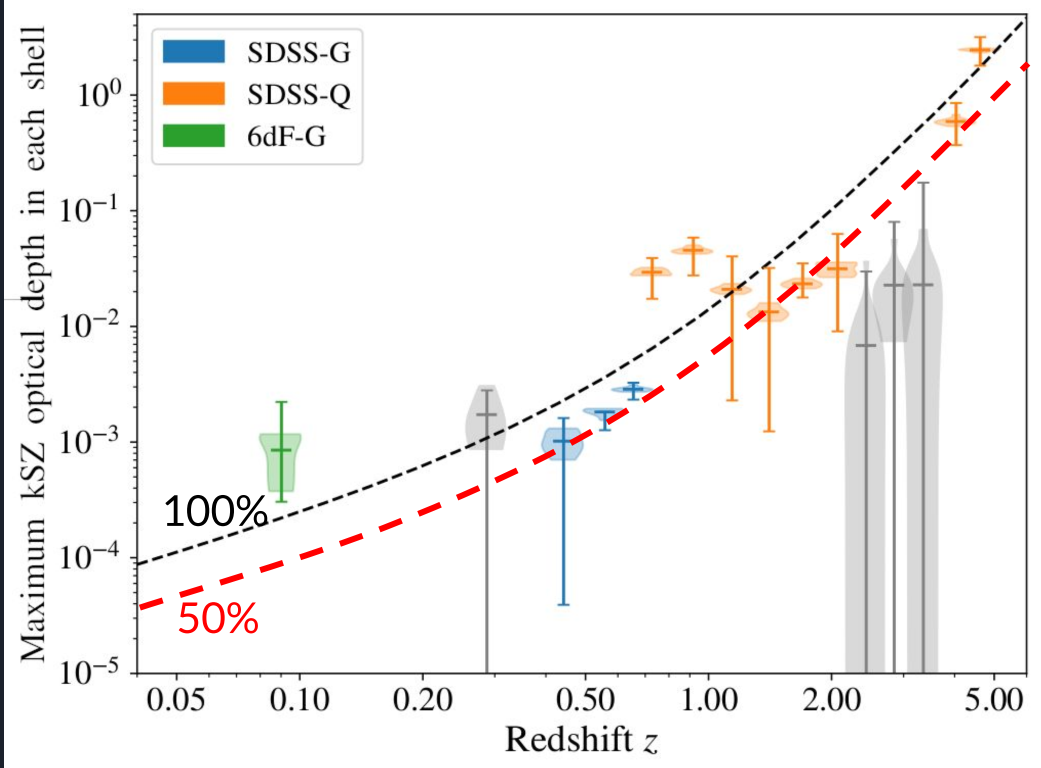

Chaves-Montero+2021

Inferring the properties of kSZ gas

We leverage kSZ optical depth measurements from different apertures at the same redshift to set constraints on the properties of kSZ gas

$$\tau^{\mathrm{th}}_{\mathrm{AP}}\left(\theta_{\mathrm{AP}}\right) = \tau\left(0,\, \theta_{\mathrm{AP}}\right) - \tau\left(\theta_{\mathrm{AP}},\, \theta_{\mathrm{AP}}\sqrt{2}\right),$$

$$\text{where} \quad \tau(x, y) = 2\sigma_T \bar{n}_{e,0} \theta_{\mathrm{AP}}^{-2} \int_x^y \theta \, \mathrm{d}\theta \int \mathrm{d}l \, \Delta_{\mathrm{gas}}(r)$$

Bayesian inference to set constraints on the parameters controlling the distribution of gas surrounding tracers, $\Delta_{\mathrm{gas}}(r)$

Properties of kSZ gas

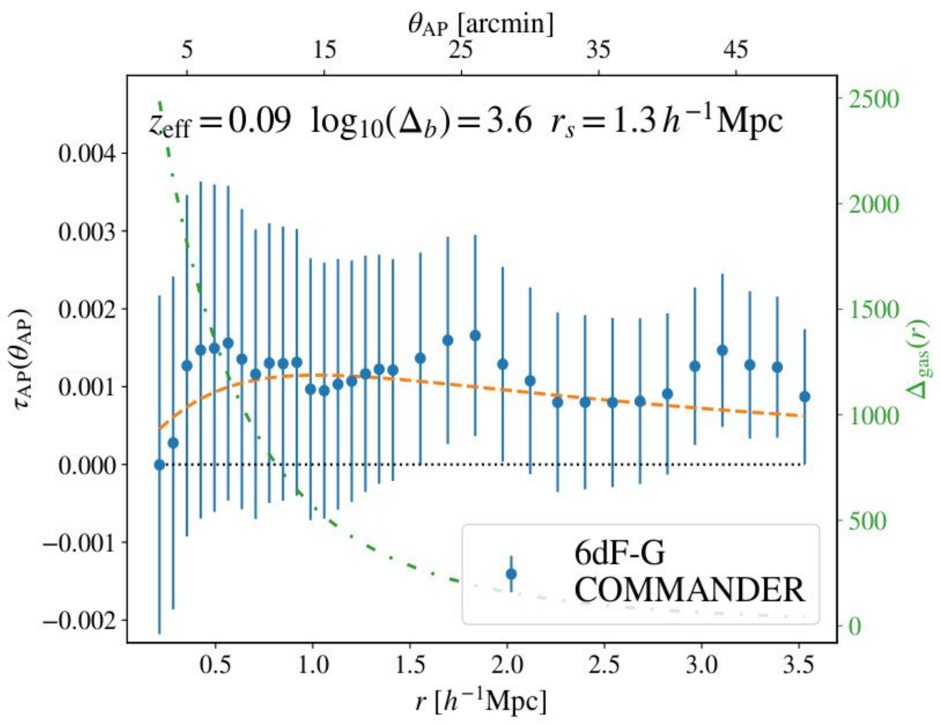

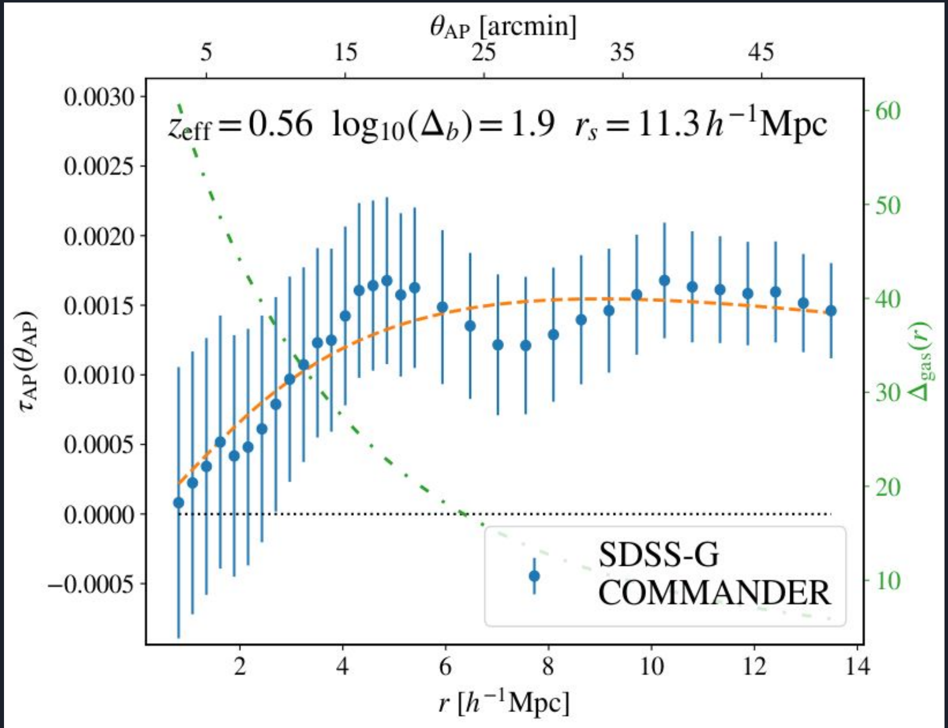

Chaves-Montero+2021

Location and density of kSZ gas

More than 99% of the kSZ gas resides outside dark matter halos

The average density of this gas ranges from 10 to 250 times the cosmic average

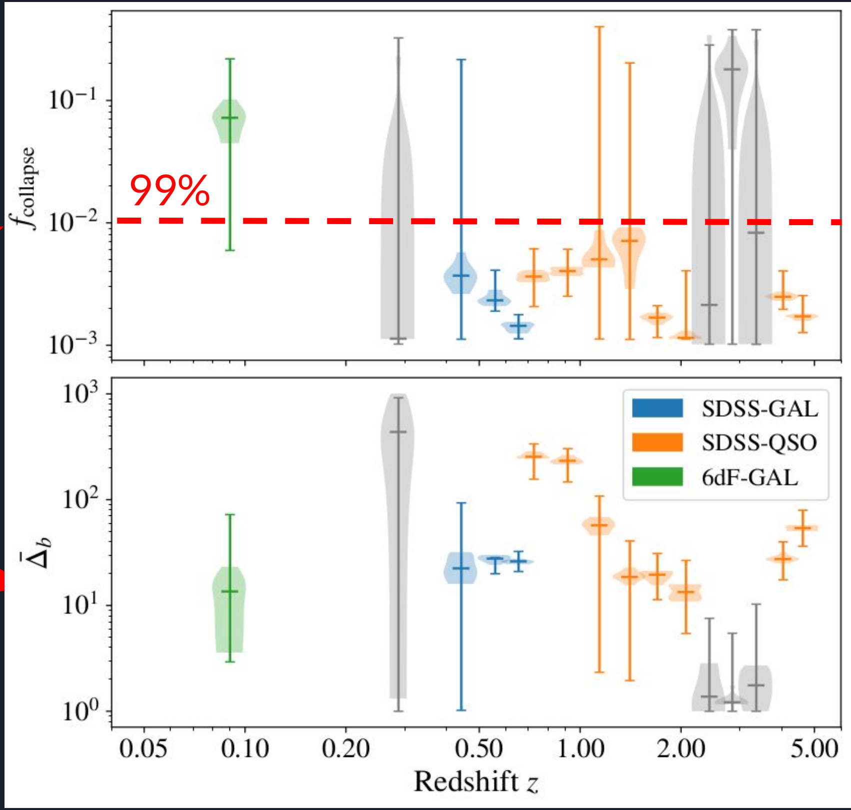

Chaves-Montero+2021

Abundance of kSZ gas

ARF-kSZ tomography is sensitive to nearly half of cosmic baryons

$$f_b \equiv \frac{\Omega_b}{\Omega_b^{\mathrm{fid}}}$$

By combining this fraction with that in halos, the early and late time abundance of baryons comes into agreement

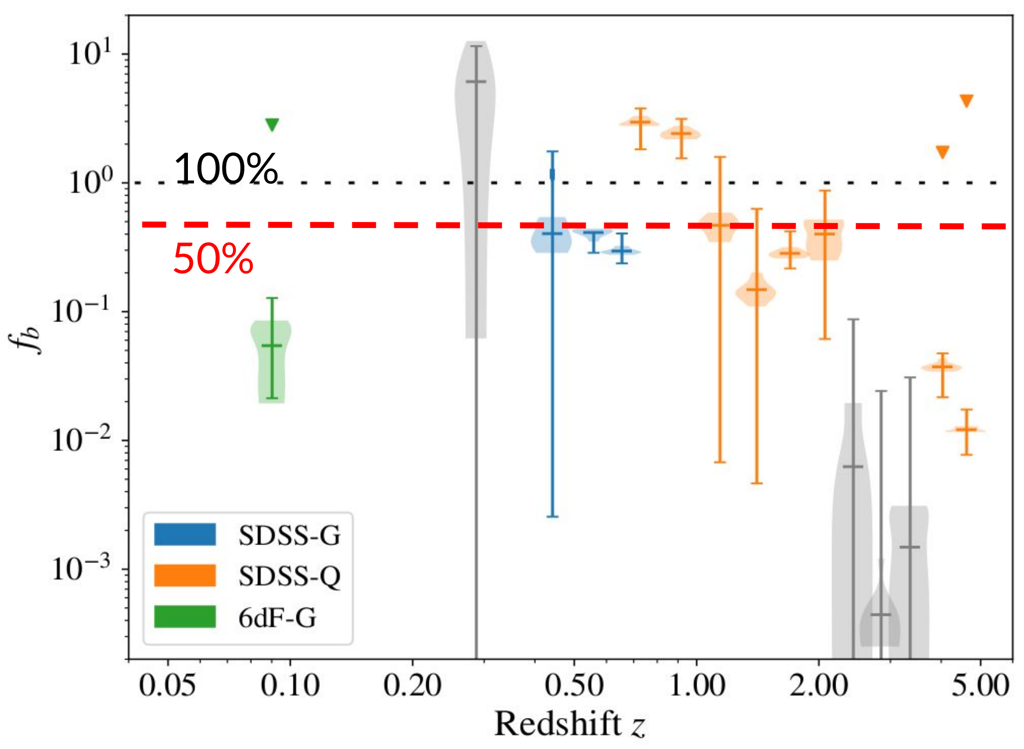

Chaves-Montero+2021

Abundance of kSZ gas

Number density of tracers

ARF-kSZ tomography is sensitive to nearly half of cosmic baryons

$$f_b \equiv \frac{\Omega_b}{\Omega_b^{\text{fid}}}$$

By combining this fraction with that in halos, the early and late time abundance of baryons comes into agreement

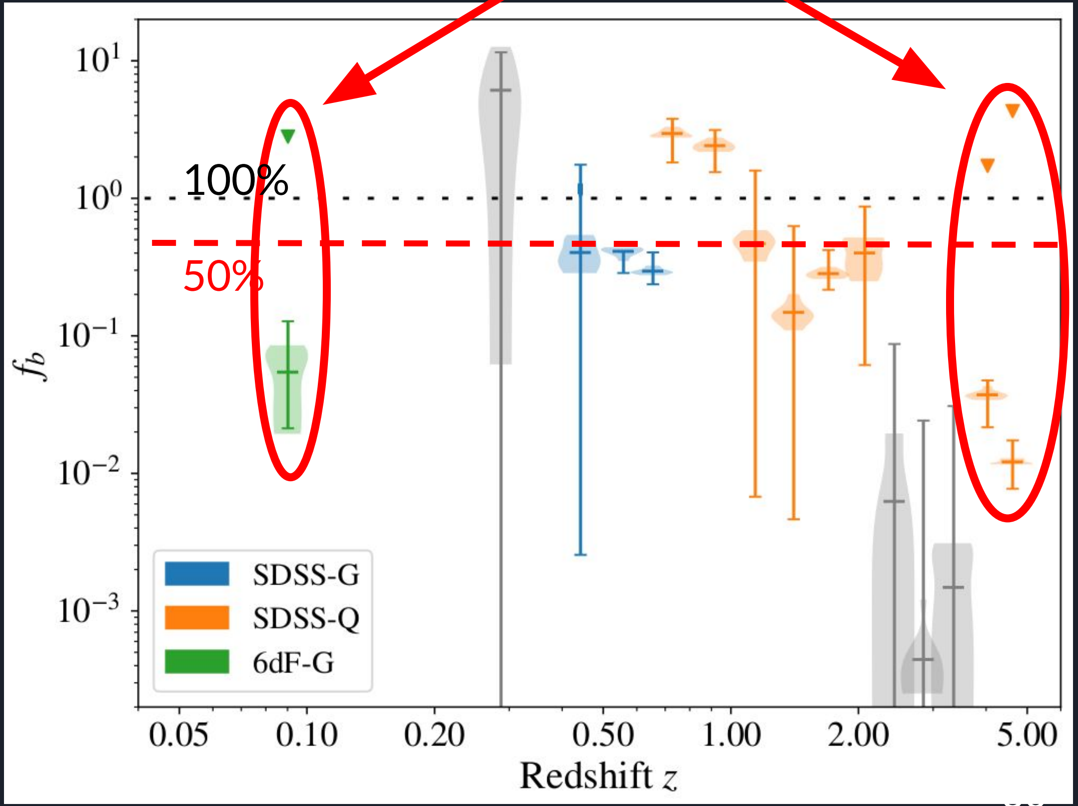

Summary

Cross-correlation of ARF maps and high-pass filtered CMB maps to detect the kSZ effect: substantial detection from z=0 to 5

kSZ measurements from different apertures at the same redshift to set constraints on the properties of kSZ gas. kSZ gas resides in the intergalactic medium and accounts for nearly half of cosmic baryons

Together with baryons in and surrounding galaxies, the amount of baryons detected via ARF-kSZ tomography is compatible with CMB+BBN results

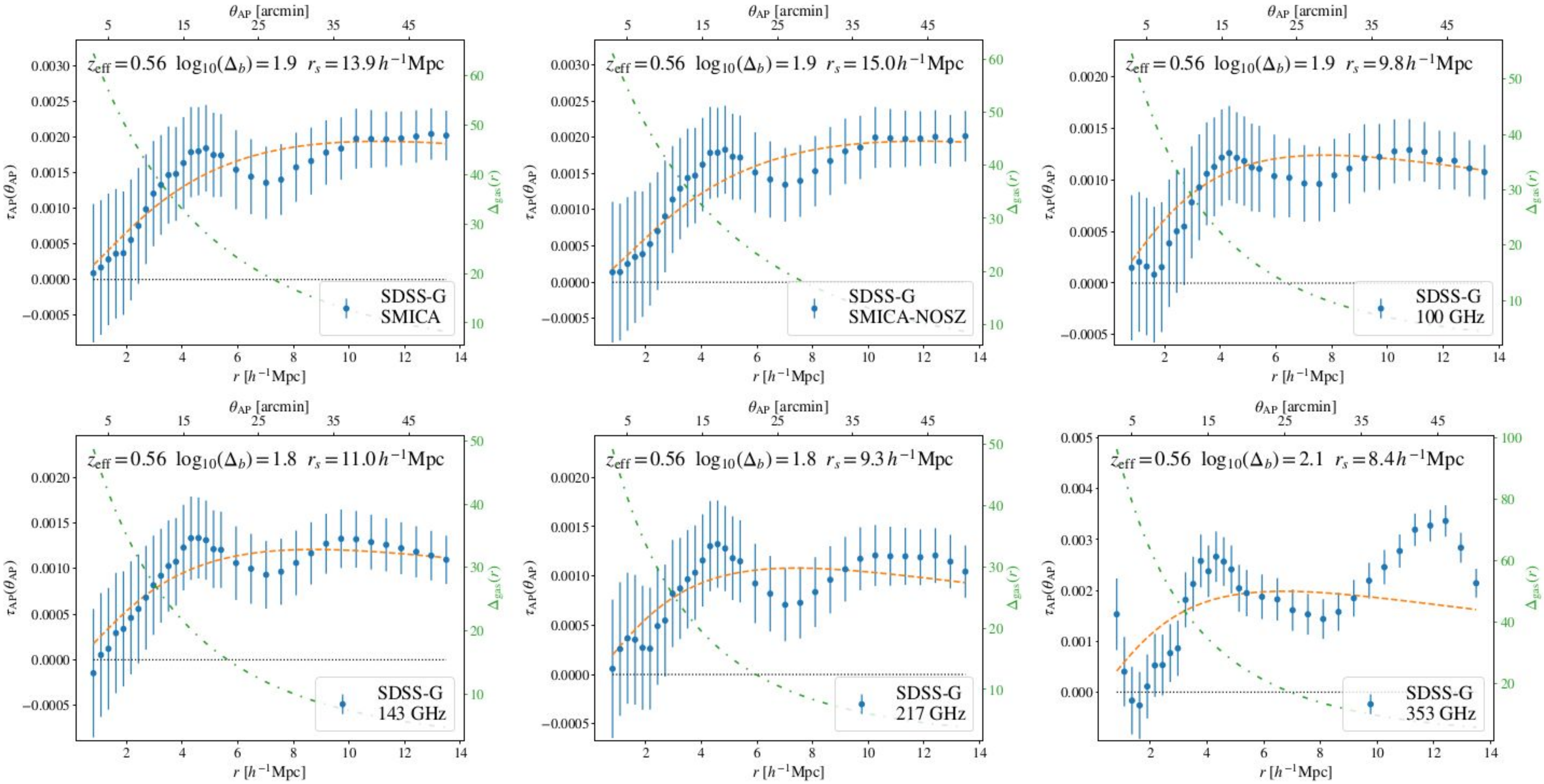

$z_{\rm eff} = 0.56$ $\log_{10}(\Delta_b) = 1.9$ $r_s = 13.9\,h^{-1}$Mpc
SDSS-G SMICA
$z_{\rm eff} = 0.56$ $\log_{10}(\Delta_b) = 1.9$ $r_s = 15.0\,h^{-1}$Mpc
SDSS-G SMICA-NOSZ
$z_{\rm eff} = 0.56$ $\log_{10}(\Delta_b) = 1.9$ $r_s = 9.8\,h^{-1}$Mpc
SDSS-G 100 GHz
$z_{\rm eff} = 0.56$ $\log_{10}(\Delta_b) = 1.8$ $r_s = 11.0\,h^{-1}$Mpc
SDSS-G 143 GHz
$z_{\rm eff} = 0.56$ $\log_{10}(\Delta_b) = 1.8$ $r_s = 9.3\,h^{-1}$Mpc
SDSS-G 217 GHz
$z_{\rm eff} = 0.56$ $\log_{10}(\Delta_b) = 2.1$ $r_s = 8.4\,h^{-1}$Mpc
SDSS-G 353 GHz
$\theta_{\rm AP}$ [arcmin]
$\tau_{\rm AP}(\theta_{\rm AP})$
$\Delta_{\rm gas}(r)$
r [h^{-1}Mpc]

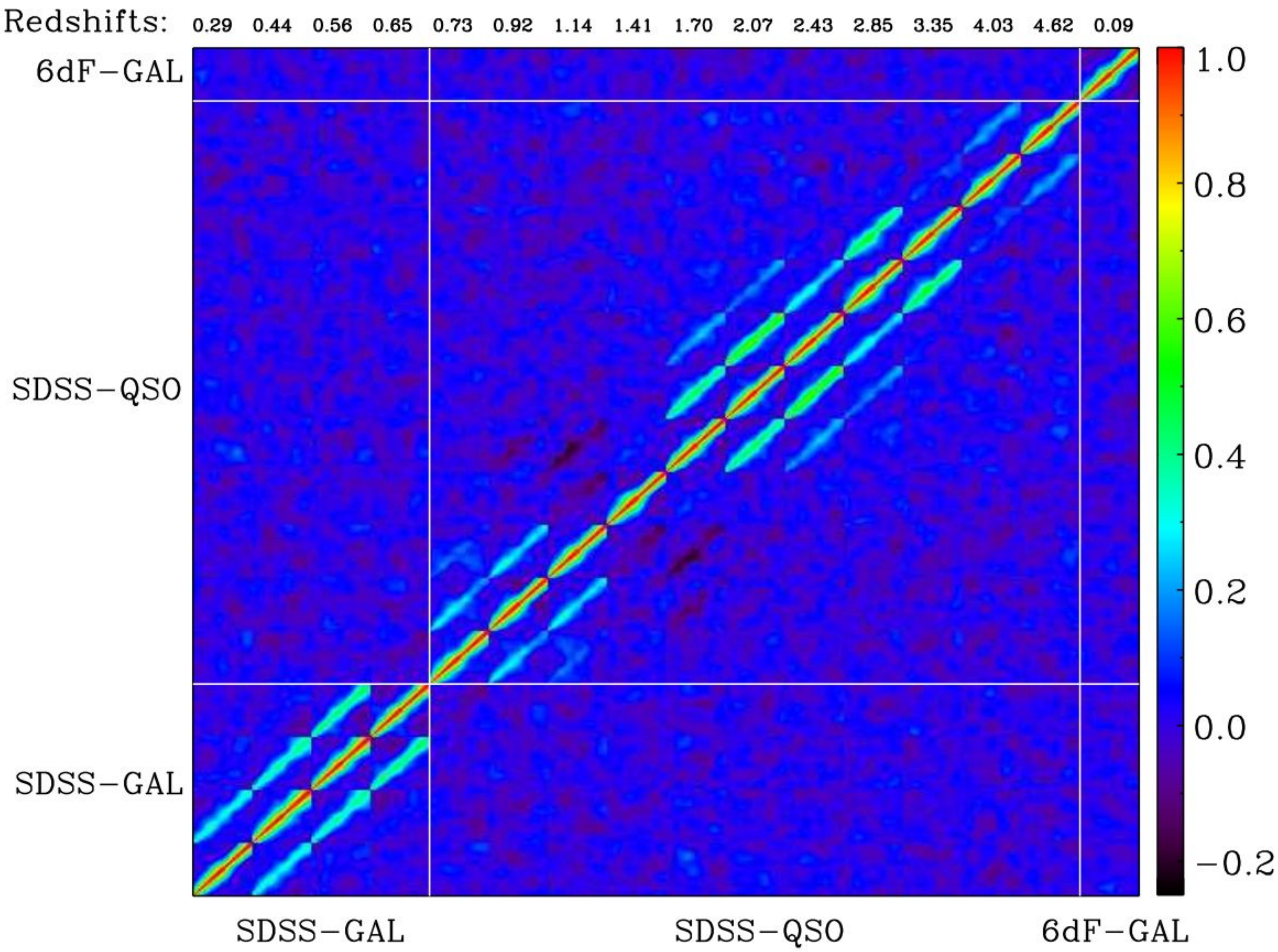
Redshifts: 0.29 0.44 0.56 0.65 0.73 0.92 1.14 1.41 1.70 2.07 2.43 2.85 3.35 4.03 4.62 0.09
6dF−GAL
SDSS−QSO
SDSS−GAL
SDSS−GAL
SDSS−QSO
6dF−GAL
1.0
0.8
0.6
0.4
0.2
0.0
−0.2

Functional form of kSZ gas distribution